Available online at www.sciencedirect.com
SCIENCE DIRECT®
European Journal of Mechanics B/Fluids 23 (2004) 587–599

Characterization of low-speed streaks in the near-wall region of a turbulent boundary layer

B. Lagraa *, L. Labraga, A. Mazouz

Laboratoire de mécanique et d'energétique, Université de Valenciennes, 59313 Valenciennes cedex 9, France

Received 2 April 2003; received in revised form 17 November 2003; accepted 19 December 2003

Available online 9 April 2004

Abstract

The low-speed streaks occurring in the near wall region of a turbulent boundary layer have been studied by means of two nonintrusive experimental techniques: the electrochemical method for the wall shear stress measurements, and the Laser Doppler Anemometer (LDA) for the velocity measurements. Correlations between the wall shear stress simultaneously measured at several points in the spanwise direction, and the correlations between the velocity and the wall shear stress simultaneously measured, indicate that in the near-wall region $y^+ < 10$ the dimensionless spanwise streak spacing is nearly constant with a value of $\lambda^+ = 110$ and increases with distance from the wall for $y^+ > 10$. These correlations also show the presence of a double-peak in the correlation curves indicating the existence of structures $\pm 6°$ tilted in (x, z) plane.

List of symbols

A	electrode area
C	concentration
C_0	bulk concentration
D	molecular diffusivity
F	Faraday constant
I	electrical current
K	mass transfer coefficient
K^+	Sherwood number: $K\ell/D$
ℓ	characteristic dimension of the electrochemical probe
$R_{u\tau}(\mathrm{T})$	correlation coefficient between u and τ: $\overline{u(t)\tau(t+T)}/u'\tau'$
Re_δ, Re_θ	Reynolds numbers: $Re_\delta = U\delta/\nu$; $Re_\theta = U\theta/\nu$
S	velocity gradient at the wall
S^+	dimensionless velocity gradient: $S\ell^2/D$
t, T	time
T^+	dimensionless time: TU_τ^2/ν
U	streamwise velocity
U_c	convection velocity
U_τ	friction velocity

* Corresponding author.
E-mail address: lagraab@yahoo.fr (B. Lagraa).

0997-7546/$ – see front matter
doi:10.1016/j.euromechflu.2003.12.005

δ boundary layer thickness
δ^* displacement thickness
θ momentum thickness
ν kinematic viscosity
τ wall shear stress

1. Introduction

Various researches undertaken over the last decades on turbulence structures have shown that the turbulent movement in the wall vicinity is not completely random but composed of organized coherent structures. Numerous types of coherent structures have been proposed to explain experimentally the phenomena observed within turbulent boundary layers such as 'bursting' process, which is accountable for most turbulent production near the wall. The various coherent structures proposed differ in their geometry, strength and orientation and notably in their evolutionary dynamics.

The streaky structure was first identified by Hama [1] by using flow visualization. It consists of alternating zones of high and low-speed fluid, extending into the logarithmic region. Low-speed fluid streamwise filaments feature a fairly uniform transverse spacing, which has been quantified and correlated by Runstadler et al. [2]. Since them, the streaky structure has been examined by different authors and for a number of different experimental conditions. Using space–time correlations, Bakewell and Lumley [3], have shown the existence of pairs of counter-rotating vortices aligned in the streamwise direction by using the proper orthogonal decomposition. Using hydrogen bubbles, Kline et al. [4], observed an intermittent streaky structure in the spanwise direction. They also found that the low-speed streaks lift away from the wall and interact with the outer flow fluid. This interaction is quite sudden and a considerable amount of turbulence production occurs during this sequence, which is referred to as 'bursting'. Kim et al. [5] have also shown the importance and the contribution of low-speed streaks in the production of turbulent kinetic energy by the process of 'bursting'. They suggested that the whole turbulent production occurs during bursting times in the $0 < y^+ < 100$ region.

The physical characteristics of the low-speed streaks such as mean transverse spacing, and vertical and streamwise extent have been examined in various studies. Gupta et al. [6], using hot wire measurements found a mean transverse spacing λ between streaks of about $100\nu/u_\tau$. This result agreed with those found by Kline et al. [4]. The same result was confirmed thereafter by Wallace et al. [7], Kreplin and Eckelmann [8], and Smith and Metzler [9]. Smith and Metzler [9] showed that the streak spacing increases with the distance from the wall. The authors carried out the visualizations of the streak structure using a high-speed video system and hydrogen bubble-wire flow visualization located normal to the flow at a $y^+ = 5$ distance of above the wall. They showed that the streak spacing appears to increase for $y^+ > 10$. These results confirm those found by Schraub and Kline [10] and Nakagawa and Nezu [11].

The presence of the streamwise vortices in near-wall turbulence is now commonly accepted [3,12,13].

Blackwelder and Eckelman [12], using a combination of hot-film probes and flush-mounted surface element and associated VITA and quadrant analysis suggested that counter-rotating streamwise vortices with a streamwise length of 1000 wall units are dominant. The same results were found by Kreplin and Eckelmann [8] and Oldaker and Tiederman [14].

By using an approach similar to that of Townsend (1979) and Mumford (1982), Stretch [13] found, from pattern eduction studies of the Kim, Moin and Moser data [15], that the predominant vortex structure in the near-wall region consists of staggered quasi-streamwise vortices. Horseshoe vortices and packets of such vortices are also observed in turbulent flows (Adrian et al. [16]).

Although the presence of streamwise vortices in near-wall turbulence is now well accepted, their evolutionary dynamics still remain an unresolved issue. Jiménez and Moin [17] who studied a channel flow in a minimal domain size, observed that the self-sustained turbulence is linked to the quasi-streamwise vortices, and does not depend on the outer part of the flow. One of the studies confirming this idea was that of Hamilton et al. [18], who studied the regeneration and dynamics of near-wall longitudinal vortices usi ng Direct Numerical Simulations of a plane Couette flow with periodic streamwise and spanwise boundaries. They showed that the turbulence structures in this minimal Couette flow were found to undergo a temporarily quasi-cyclic process of regeneration and that this process is composed of three distinct phases: building up streaks by streamwise vortices, streaks breakdown, and streamwise regeneration vortices.

Recent promising developments concerning the near-wall portion of the inner layer, have focused on the role of the low-speed streaks and have demonstrated that the well-resolved wave solutions of the Navier–Stokes equations capture the essential structural and statistical features of turbulent shear flows (Waleffe [19], Jeong et al. [20]) among others. In particular, Jeong et al. [20] developed a conceptual model to explain observed kinematic features for the educed coherent structure details. This near-wall coherent structure model consists of a train of elongated quasi-streamwise vortices, inclined 9° in (x, y) and tilted $\pm 4^\circ$ in (x, z), with vortices of alternating sign overlapping in x as a staggered array. These theories and models rest upon studies of near-wall structure using experiments and low-Reynolds number direct numerical simulation (DNS).

Labraga et al. [21], using simultaneous measurements of the velocity and the shear stress, showed that the inclination of the coherent structures in the (x, y) plane depends on the distance from the wall. They suggested that, in the vicinity of the wall, the inclination is about 5° and is 15° in the outer region. Wietrzak and Lueptow [22], measured instantaneous streamwise fluctuations of the wall shear stress using a hot-element probe in a thick axisymmetric turbulent boundary layer on a cylinder aligned parallel to the flow. The cross-correlation curves of the wall shear stress simultaneously measured at two points in the spanwise direction show the presence of a double peak as the probes are spaced further apart. The maxima of the double peaks occur at greater T^+ as the distance between the probes increases, supporting the idea of a structure yawed to the cylinder axis. Wietrzak and Lueptow [22] suggested that the yawed structures could feature an arrowhead or half-arrowhead shape and may be associated with fluid from outer flow washing over the cylinder. The simultaneous measurements of the wall shear stress in planar wall-bounded flows using multiple shear stress probes separated by a spanwise distance were made by Mitchell and Hanratty [23], Blackwelder and Eckelmann [12], Kreplin and Eckelmann [8] and Nikolaides et al. [24]. Kreplin and Eckelmann [8], who studied the correlation between the signals from the shear probes, did not observe double peaks in their correlation analysis. This is mainly due to the experimental techniques that suffer from a lack of spatial resolution.

It is shown from this brief review that numerous studies have dealt with the low speed structures' characteristics. However, owing to the lack of their spatial resolution or to their intrusive character, the different experimental techniques often used were not able to sense some geometrical features of coherent structures in near-wall turbulence. The knowledge of these organized motions is paramount for a better understanding of the bursting process and for a turbulent boundary layer's large scale control strategy. The aim of this study is to contribute to a better knowledge of the near-wall turbulent structures by simultaneous measurements of the fluctuating wall shear stress and the streamwise velocity respectively by the electrochemical technique and laser Doppler anemometry. Both measurement techniques are non-intrusive and yield valuable information in the near wall region of a turbulent boundary layer.

2. Electrochemical method measurement

2.1. Principle

The electrochemical technique, widely described by Reiss and Hanratty [25], consists of measuring the limiting current at the cathode of an electrolysis cell during an electrochemical reaction, so as to determine the mass transfer rate under conditions for which this reaction rate is high enough so that the concentration of the reacting ions may be considered nul at the surface of the small working electrode. An example of an electrochemical cell using a potassium ferricyanide–ferrocyanide red-ox couple is shown in Fig. 1(a). The current involved by the chemical reaction depends on four phenomena: molecular diffusion, forced and natural convection, migration in the potential field. The natural convection is negligible when the reduced wall shear stress S^+ is high enough. We can suppress the migration by the addition of excess neutral electrolyte in the solution so that the transfer of the active species from the bulk of the flow is only governed by forced convection. In these conditions the mass balance equation is:

$$\frac{\partial C}{\partial t} + u\frac{\partial C}{\partial x} + v\frac{\partial C}{\partial y} = D\frac{\partial^2 C}{\partial y^2}, \tag{1}$$

where u and v are the components of the velocity, D the diffusion coefficient and C the concentration of the active ions.

Under these circumstances, the current I flowing to the test electrode of area A is related to the mass transfer coefficient K by:

$$K = \frac{I}{An_{\mathrm{e}}FC_0}, \tag{2}$$

where n is the number of electrons involved in the reaction, F the Faraday's constant and C_0 the bulk concentration of active species. Since the system is characterized by a large Schmidt number, the concentration boundary layer is thin and the velocity field within the concentration boundary layer may be characterized by the following relationship:

$$U = Sy, \tag{3}$$

where S is the mean velocity gradient at the wall and y the distance from the wall, Fig. 1(b).

If the dimensionless velocity gradient at the wall $S^+ = S\ell^2/D$ (ℓ: electrode length, D: diffusion coefficient) is sufficiently high, it is possible to neglect the longitudinal diffusion and a solution of the steady-state mass balance equation therefore gives:

$$\frac{K\ell}{D} = c\left(S^+\right)^{1/3}. \tag{4}$$

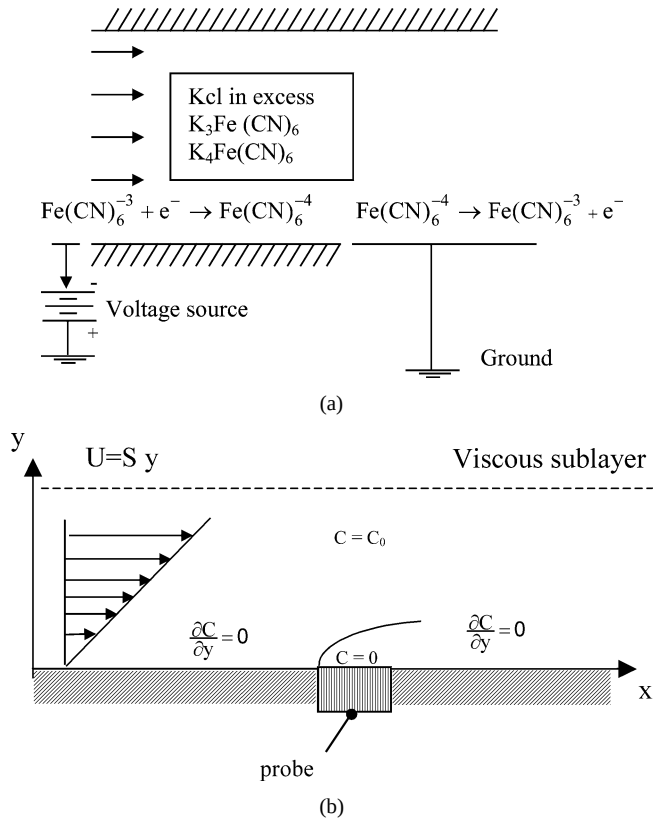

Fig. 1. (a) Electrochemical cell. (b) Concentration field and velocity profile over an electrochemical probe.

The integration of the mass transfer equation by several authors provides a theoretical value for the c coefficient in the case of a rectangular probe, $c = 0.807$. The dimensionless form of Eq. (4) is used for unsteady flows starting from the assumption that the variation of the wall shear rate is very slow.

2.2. Frequency response of electrochemical probes

In the case of unsteady flows featuring low velocity variations, Hanratty and Campbell [26] proposed a pseudo-steady state assumption allowing the use of the one-third power law to calculate the instantaneous wall shear rate. However, in many cases, the concentration boundary layer inertia cannot be neglected and the quasi-steady state assumption is not valid. In the case of the dynamic behavior of electrochemical probes, most investigations assume that the shear rate fluctuation amplitude is small as compared to the time averaged shear rate. With this assumption, the mass balance equation can be linearized and solved both analytically [23,27] and numerically [28–30]. Therefore, the transfer function between the mass flux and the wall shear rate at different frequencies can be deduced. The difficulty of this approach is that the linearization assumption is not always valid. The direct correction of the electrochemical signals seems to be quite an attractive method to solve the issue of the dynamic behavior of the electrochemical probe. An approximate solution suggested by Sobolik et al. [31], enables the restoration of the wall shear stress in the time domain in unsteady flow conditions. They proposed an approximate solution that may be expressed as follows:

$$S_c(t) = S_{qs}(t) + \frac{2}{3} t_0 \frac{\partial S_{qs}}{\partial t}, \tag{5}$$

where the first term on the RHS of Eq. (5) corresponds to the quasi-steady solution and the second term represents the inertial effect. In the present study, the characteristic time of the probe, t_0, was experimentally obtained by using a transient voltage-step. An example is given in Fig. 2 where the experimental data are obtained by turning a probe from off to on at a steady shear rate, generating therefore a voltage-step. Fig. 2 corresponds to the second law Fick's solution that may be written as follows:

$$I(t) = \alpha t^{-1/2} \tag{6}$$

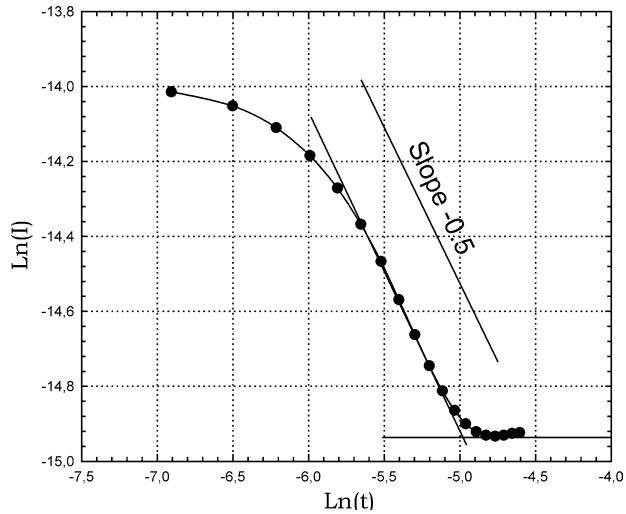

Fig. 2. Determination of the characteristic time t_0 by the transient voltage-step.

with

$$\alpha = n_e F C_s A \left(\frac{D}{\pi}\right)^{1/2}. \tag{7}$$

This method permits to determine the electrochemical probe active surface when the diffusion coefficient D and the bulk concentration C_0 are known.

The characteristic time t_0 corresponds to the intersection of asymptotic parts of the current response to the transient step change of the polarization (Wein [32]). This method used to correct the electrochemical signals, taken in a turbulent boundary layer, provides satisfactory results. Therefore it is applied here to restore the instantaneous wall shear stress. More details are given in [21].

3. Experimental details and procedure

The experiments were carried out in a perspex water-channel. The test section is 0.15 m by 0.15 m and is 1.5 m long. The boundary layer was tripped by three-dimensional roughness elements flush with the wall, in order to achieve a turbulent regime at the measurement section located 1.10 m downstream of the trip. The pressure gradient along the test section was negligible.

The electrolyte is a dilute solution containing 1.7 mol m^{-3} potassium ferricyanide, 1.4 mol m^{-3} potassium ferrocyanide and potassium chloride in a concentration of 400 mol m^{-3}. Ferrocyanide oxidization was chosen because of the large range of voltage over which the current is mass transfer controlled, and above all, because the electrochemical solution is transparent and therefore allows LDV measurements. When a voltage difference is imposed across the electrode, the following reaction occurs at the cathode with the reverse reaction at the anode:

$$\mathrm{Fe(CN)}_6^{3-} + e \rightarrow \mathrm{Fe(CN)}_6^{4-}.$$

A circular platinum electrochemical probe was flush mounted onto the upper wall of the test section channel for the wall shear stress measurements. Its diameter is 0.17 mm, corresponding to 7.4 viscous lengths. An array of 25 electrochemical probes was used to identify the coherent structures within the viscous sublayer. The spanwise separation between two probes was 0.2 mm corresponding to 9 viscous lengths.

Measurements relative to the U-component velocity are performed using a 4 W argon-ion laser in backscatter mode. A TSI Model 9201 ColorBurst multicolor beam separator is used to split the beam and its frequency shifted counterparts are passed to a 2-component, TSI Model 9832 probe through a fiber-optic cord. Probe beam spacing is 50 mm, and lenses with focal lengths of 120 mm and 350 mm are available. The dimensions of the measuring volume in the present study are $0.05 \times 0.05 \times 0.32$ mm^3, which corresponds to $2.35 \times 2.35 \times 15$ wall units.

A datalink system allows the electrochemical analog signal to be acquired and stored simultaneously with the LDV velocity data. The signals provided from the electrochemical array probe analyzed and discussed in section 4.3 were sampled at 500 Hz

Table 1
Turbulent boundary layer mean characteristics

U ($m\,s^{-1}$)	δ (mm)	δ^* (mm)	θ (mm)	R_δ	R_θ	U_τ ($m\,s^{-1}$)
1.1	21	3.100	2.215	27,176	2,860	0.047

after being low-pass filtered at 250 Hz. The data were digitized using a 12 bits CELI-SAB A/D board in a personal computer. The temporal sampling record was $2000\delta/U$ corresponding to 20000 points.

The basic flow and measurement parameters are plated in Table 1. Further details of the experiments are given in [33].

4. Results and discussion

4.1. Spanwise spacing of low-speed streaks

The electrochemical signals are initially corrected using the approximate integral method to avoid the problem of the probes frequency response.

Here, the low-speed streak spacing has been estimated by means of the space–time correlations between velocity and wall shear stress, simultaneously measured. The principle is to maintain the electrochemical probe in a fixed position and to move the measuring volume along the (y, z) plane. The space–time correlation coefficient is defined by:

$$R_{\tau u}(T, z) = \frac{\overline{\tau(t, z)u(t + T, z + \Delta z)}}{\tau'(z)_{\mathrm{rms}} u'(z + \Delta z)_{\mathrm{rms}}},$$

where τ is the wall shear stress; u, the streamwise velocity; T, the time delay between the signals.

Figs. 3(a)–7(a) show the correlation between the velocity and the wall shear stress when the measurement volume is moved spanwise at different distances from the wall. The magnitude of the correlation coefficient is nearly one near the wall when the velocity measurement volume is located directly above the electrochemical probe, suggesting a strong correlation. The magnitude of the correlation decreases as the velocity probe is moved farther from the electrochemical probe.

For a given spanwise distance, the time shift corresponding to the peak value of the correlation coefficient increases with distance from the wall, indicating that the structure is inclined to the wall in the streamwise direction as was widely discussed by numerous authors (Adrian et al. [16], Lagraa [33]).

The half low-speed streak spacing will be indicated by the passage of the curve of spatial correlation by a minimum. The space–time correlations and the spatial correlation curves near the wall at $y^+ = 2, 5$ are represented in Fig. 3 and at $y^+ = 10$ in Fig. 4. The spatial correlation curves reach their minimum at the point where the transverse spacing between the two probes is $\Delta Z^+ = 55$ indicating that in the $y^+ < 10$ region, the low-speed streak spacing value is about $\lambda^+ = 110$. This result corroborates those given by the experiments as well as simulations at low Reynolds numbers [4,5,8,9,19].

The maxima of the correlations in, Figs. 3(a)–7(a) peak at negative time delay. This is due to the inclined features of the coherent flow structures already observed in numerous studies. This time shift is needed for the structure to travel from the location of the measurement LDV volume to the wall.

4.2. Variations in streak spacing with distance from the wall

In order to examine the behavior of the streak spacing in the buffer and logarithmic region, the correlations have been recalculated at three different wall distances: $y^+ = 15$, 30 and 50 represented respectively on Figs. 5–7. The apparent characteristic illustrated by these figures is the increased mean streak spacing for $y^+ > 10$. This behavior was underlined by some authors. By using visualizations and the correlation techniques, Schraub and Kline [10] showed that the distance between the streaks takes a constant value of $\lambda^+ = 100 \pm 20$ in the $y^+ < 7$ region and it increases with the distance from the wall for $y^+ > 7$. Also by using visualizations at low Reynolds numbers combined with the correlation techniques using measurements with a hot film, Nakagawa and Nezu [11] gave an average value of $\lambda^+ = 100$ for $y^+ < 5$ and showed that it increases with the distance from the wall beyond $y^+ = 5$. Their results appear to be in agreement with the present result (Fig. 8). For $y^+ < 10$, the streak spacing is constant and it increases with the wall distance for $y^+ > 10$. However, for $y^+ > 50$, the streak identification becomes uncertain and the low-speed steaks undergo a transformation in their shape (increasing λ^+) and consequently their nature also changes to become hairpin vortices. This result confirms the observations carried out by Smith and Metzler [9] in which the breakdown of the streak during the bursting process appeared to be associated with a formation of a series of stretched

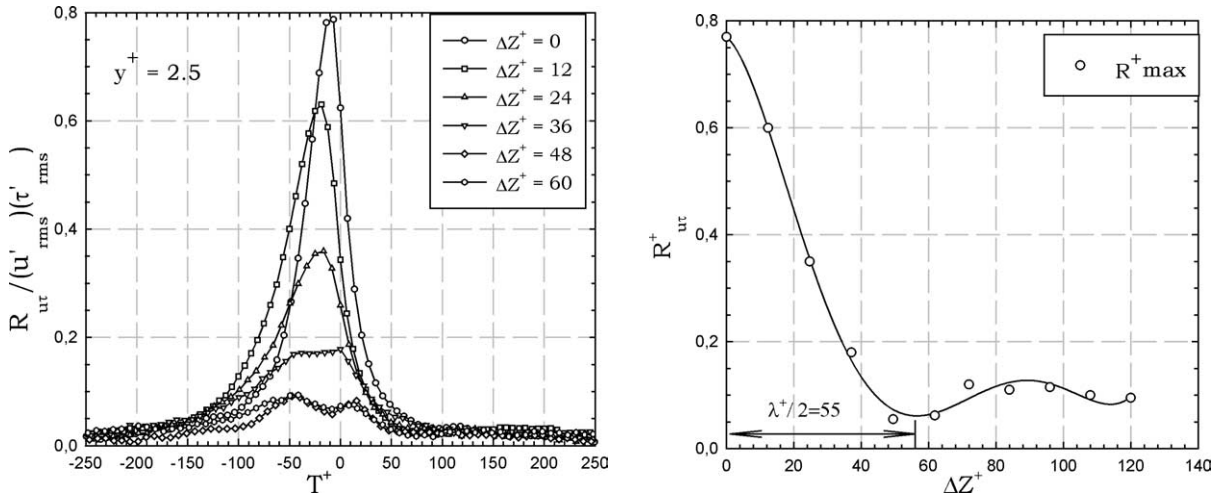

(a) (b)

Fig. 3. Correlations between velocity and wall shear stress, $y^+ = 2.5$. (a) Space–time correlations as a function of T^+ parameter ΔZ^+; (b) spatial correlations as a function of ΔZ^+ at $T^+ = 0$.

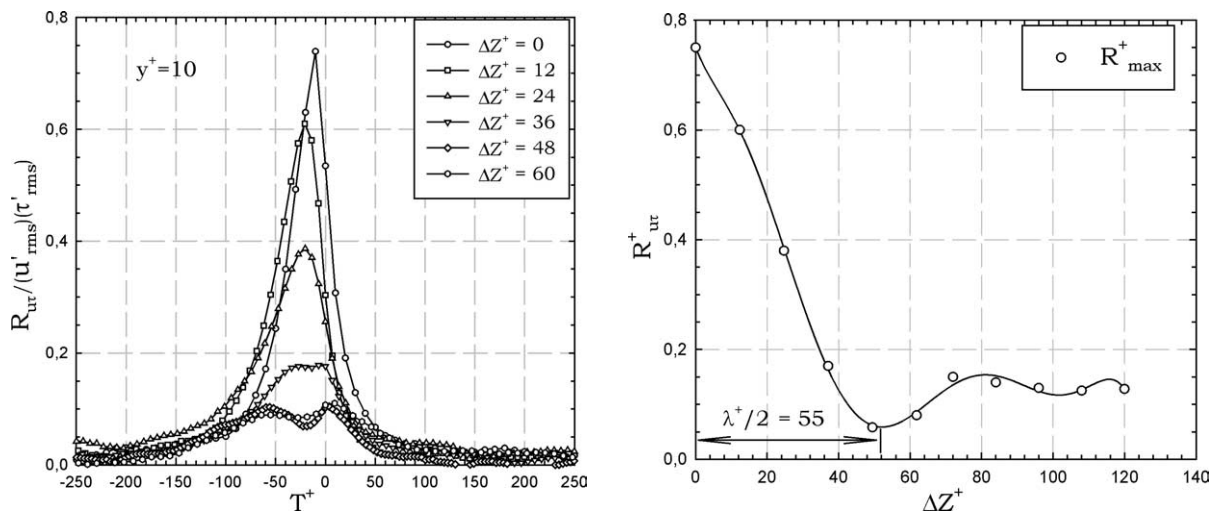

(a) (b)

Fig. 4. Correlations between velocity and wall shear stress, $y^+ = 10$. (a) Space–time correlations as a function of T^+ parameter ΔZ^+; (b) spatial correlations as function of ΔZ^+ at $T^+ = 0$.

hairpin vortices in the near wall region. The legs of the vortices appear as counter-rotating vortex pairs which pump the fluid away from the wall.

The most remarkable feature of the transverse space–time correlation is the appearance of a double peak in the correlation curves. This phenomenon depends on the measuring volume position to the wall, and on the transverse spacing between the electrochemical probe and the measuring volume. The time interval between the maxima of the double peaks occurs at a greater T^+ as the transverse spacing between the two probes increases. This indicates the different shapes of the coherent structure through the boundary layer. Indeed, in the $(2.5 < y^+ < 10)$ region, the double peaks appear only from $\Delta Z^+ = 36$ with the time interval between the two peaks increasing significantly. The double peak is either due to an arrowhead shape or to tilted structures in (x, z) plane with equally probable occurrence in either direction (Fig. 11). These structures are identified as being the quasi-longitudinal vortices that dominate this region. In the buffer region $(10 < y^+ < 30)$, the double peaks appear from $\Delta Z^+ = 48$ and in the logarithmic region $(y^+ > 50)$, from $\Delta Z^+ = 72$. These results indicate the gradual widening of the structure scale whenever the structure is moved away from the wall. This shape transformation was proposed in Smith's model

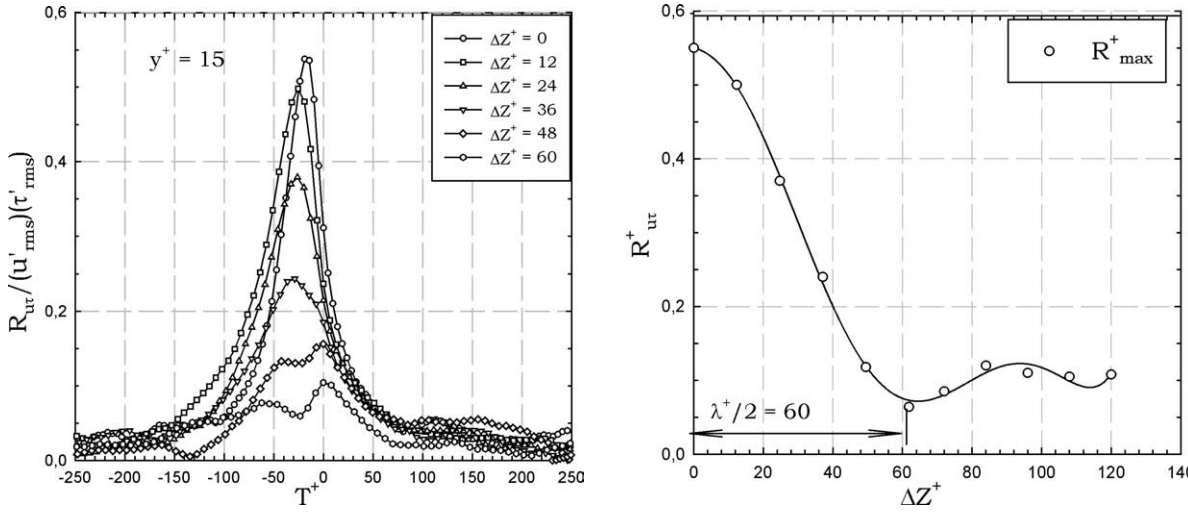

(a) (b)

Fig. 5. Correlations between velocity and wall shear stress, $y^+ = 15$. (a) Space–time correlations as a function of T^+, parameter ΔZ^+; (b) spatial correlations as a function of ΔZ^+ at $T^+ = 0$.

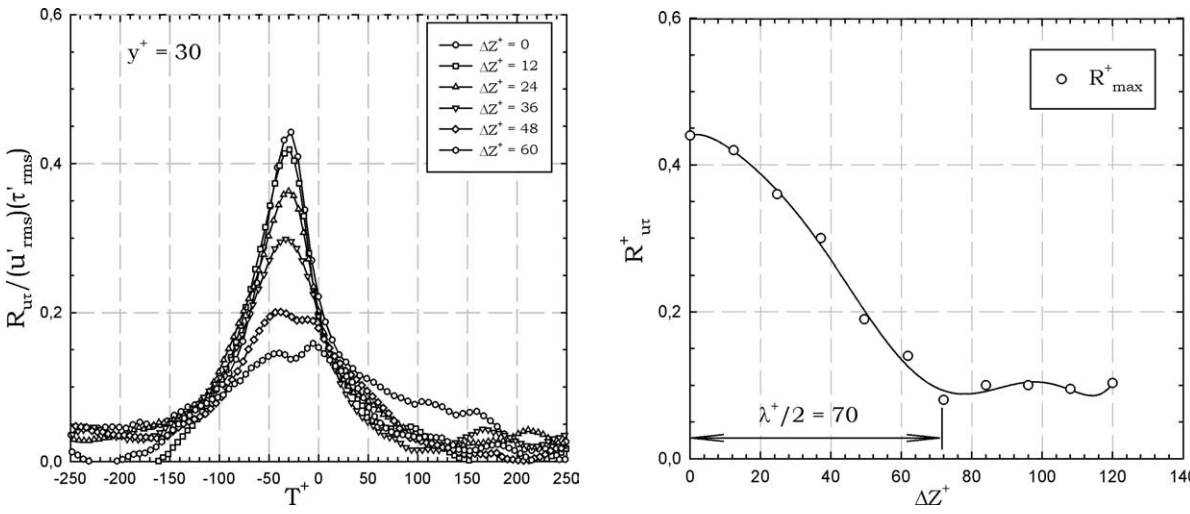

(a) (b)

Fig. 6. Correlations between velocity and wall shear stress, $y^+ = 30$. (a) Space–time correlations as a function of T^+, parameter ΔZ^+; (b) spatial correlations as a function of ΔZ^+ at $T^+ = 0$.

[34], where it was suggested that the bursting of the low-speed streaks generates the hairpin vortices. This phenomenon is also found in the model proposed by Robinson [35] who suggested that quasi-streamwise vortices dominate the buffer region, while archlike vortices are the most common vortical structure in the wake region, and in the logarithmic region both arches and quasi-streamwise vortices are to be found. Adrian [16], also showed in his model that in the buffer region, the hairpin legs are quasi-longitudinal vortices that raise the low-speed fluid.

4.3. Wall shear stress simultaneous measurements

In order to investigate the double-peak phenomenon in depth, we used a transverse array of closely spaced electrochemical probes that could measure the wall shear stress simultaneously at several points spanwise (Section 1.1). The probe at the centre of that array was taken as a reference.

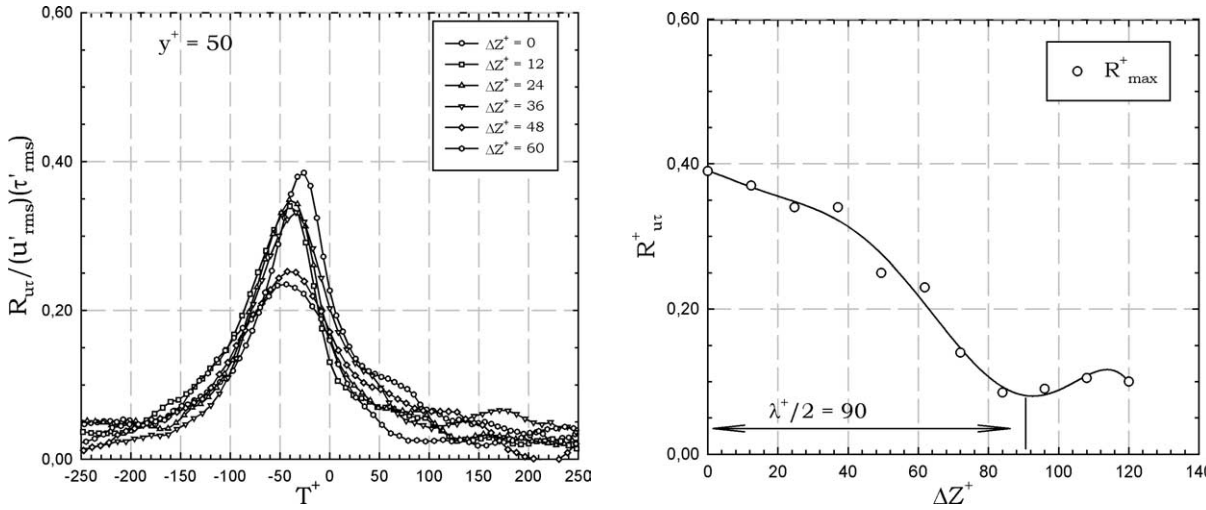

(a) (b)

Fig. 7. Correlations between velocity and wall shear stress, $y^+ = 50$. (a) Space–time correlations as a function of T^+ parameter ΔZ^+; (b) spatial correlations as a function of ΔZ^+ at $T^+ = 0$.

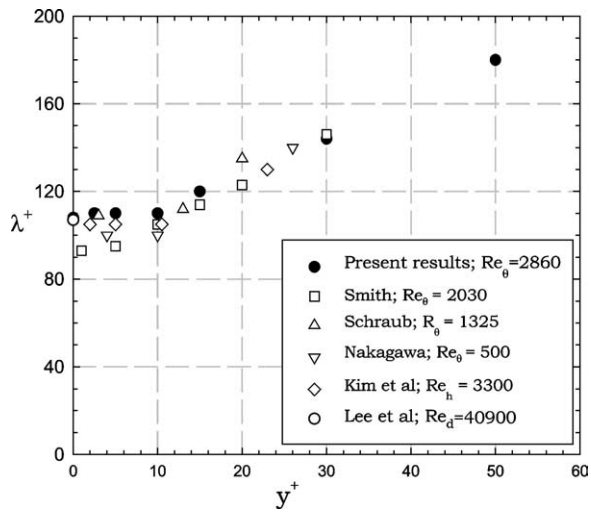

Fig. 8. Variation of mean spanwise streak spacing with distance from the wall.

The space–time correlation coefficient of wall shear stress at two points is given by:

$$R_{\tau_1\tau_2}(T, \Delta z) = \frac{\overline{\tau_1(t, z)\tau_2(t + T, z + \Delta z)}}{(\tau_1'(z))_{\text{rms}}(\tau_2'(z + \Delta z))_{\text{rms}}},$$

where τ_1 and τ_2 are the wall shear stress measured by each probe.

The spanwise correlation coefficient is shown in Fig. 9. The half spacing ($\lambda/2$) is generally estimated as the transverse distance for which the space correlation passes by a negative minimum point. Fig. 9 shows that the minimum is reached for $\Delta Z^+ = 54$ corresponding to a spanwise spacing of low-speed streaks of $\lambda^+ = 108$. This result well confirms the one found by the space–time correlations between the velocity and the wall shear stress. Lee et al. [36] measured the spanwise correlation coefficient using the electrochemical method in a turbulent pipe flow at Reynolds numbers 26 900 and 35 900. They found that an average wavelength of a large sublayer eddy structure is about $\lambda^+ = 107$, quite in excellent agreement with the present results as it is shown in Fig. 8 for $y^+ = 0$. Fig. 9 shows that the present results agree well with those found by Kim et al. [15] in their low Reynolds number simulations.

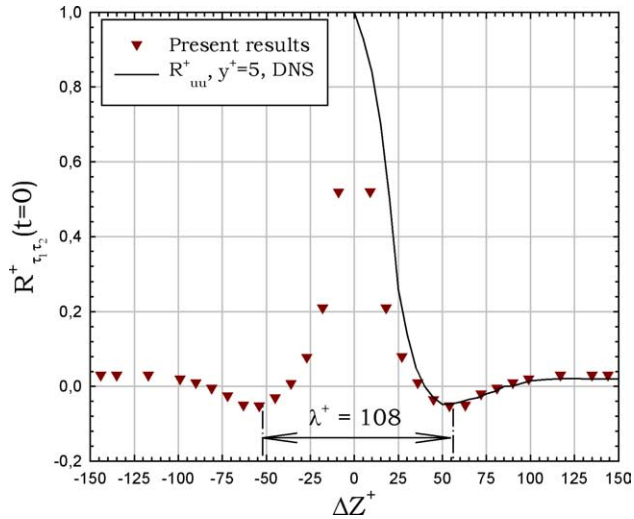

Fig. 9. Transverse spatial correlations of the wall shear stress at $T^+ = 0$.

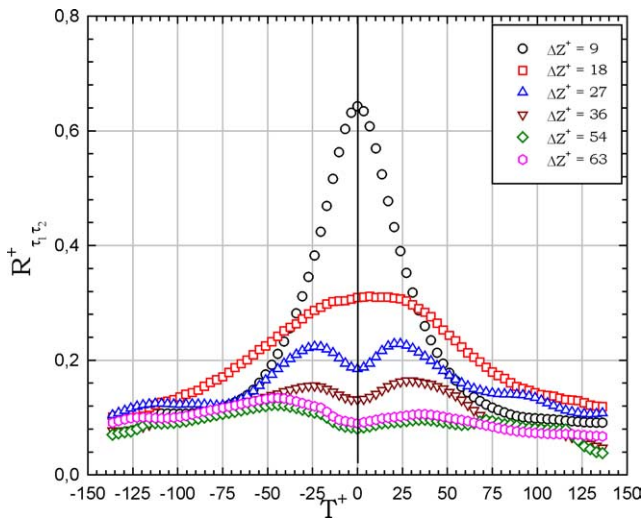

Fig. 10. Space–time correlations of the wall shear stress.

The various curves of space–time correlations are shown in Fig. 10, in which the double peaks start appearing at a transverse distance between the two probes of $\Delta Z^+ = 27$. These double peaks were already observed on the correlation curves between velocity and wall shear stress for the various positions to the wall. Their presence in the near-wall region informed us about the shape of the quasi-longitudinal structures that dominate this region. The results showed that these structures are tilted in the (x, z) plane. The β angle inclination was estimated from the spanwise separation between the two probes, the lag time of the correlation peaks and the convection velocity $U_c = 13u_\tau$ (calculated following to the procedure used by Labraga et al. [21]). A sketch illustrating the inclined structure is shown in Fig. 11.

For $\Delta Z^+ \leqslant 18$, Fig. 9 shows that the lag time corresponding to the peak value of $R_{\tau 1\tau 2}$ is zero. This means that both probes simultaneously detect the same coherent structure. For $\Delta Z^+ > 18$, the coherent structure will be detected first by probe 1 and ΔT by probe 2 later on. Meanwhile, the structure has travelled along the wall distance $\Delta X = U_c \cdot \Delta T$. This structure is responsible for the peak value of $R_{\tau 1\tau 2}$ at negative T^+. However, since the inclination of the structure is equally probable in either direction, another structure yawed at $-\beta$ angle, will generate the peak value of $R_{\tau 1\tau 2}$ at positive T^+.

The experimental uncertainties associated with the calculated angle β, are mainly due to systematic errors resulting from the estimation of the effective area of each probe and to the peak value of the correlation coefficient. The estimated uncertainty of a probe area is less than 5%. The uncertainty on the maxima of the double peak is estimated to be less than 2%. Therefore,

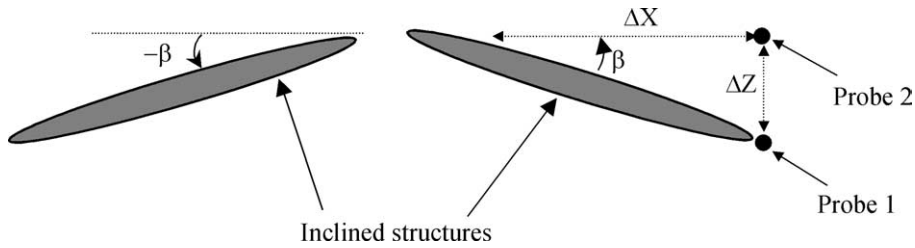

Fig. 11. Schematic of possible coherent structures responsible for the double peak in the spanwise space–time cross correlation.

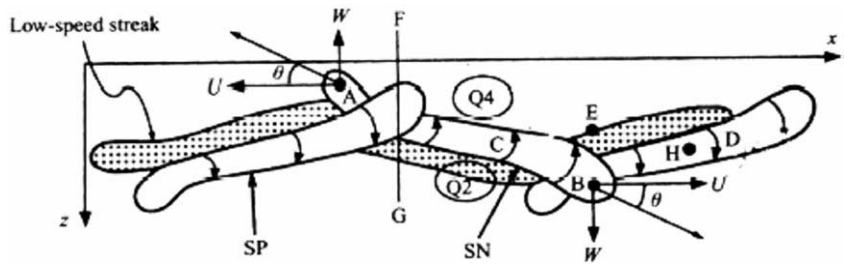

Fig. 12. Conceptual model of an array of coherent structures from Jeong et al. [20].

the experimental uncertainty in the final evaluation of β is less than 7% especially for the probe spaced of $\Delta Z^+ = 27$ for which the cross correlation is symmetric. For $\Delta Z^+ > 27$, the peaks become asymmetric and less distinctly identifiable, due to the inherent smearing of the averaging and to the difference between values of τ'_{rms} measured by both electrochemical sensors.

These results show that the structures are tilted $\pm 6°$ in the horizontal plane with a maximum spanwise extension of $\Delta Z^+ = 108$ and a head of about $\Delta Z^+ = 36$. The present results are consistent with the staggered streamwise vortices suggested by Stretch [13] and confirmed by Waleffe [19] and Jeong et al. [20].

Several researchers have made simultaneous measurements of the wall shear stress in planar wall-shear flows using several transversely spaced flush mounted probes. None of these authors, with the exception of Kreplin and Eckelmann [8], have however presented the corresponding correlation curves. The latter varied the spanwise distance between the probes in a $12.6 \leqslant \Delta z^+ \leqslant 105$ range. Their correlation curve for $\Delta z^+ = 12.6$ has a maximum at $T^+ = 0$ and is symmetric, as are the correlation curves at the other distances Δz^+ not shown in their paper. These authors neither showed nor mentioned the presence of a double peak in their correlation curves. They used hot-films flush-mounted in the wall to measure the velocity gradient at the wall. The small dimensions of their hot-films (5.4 viscous lengths) lead to a high enough spatial resolution to observe the double peak of the spanwise cross-correlation, comparing with the dimension of our probes (7.4 viscous lengths).

From direct numerical simulations of a turbulent channel flow, Jeong et al. [20] educed coherent structures by using a conditional sampling scheme which extracts the entire extent of dominant vortical structures. They showed that the coherent structures are elongated quasi-streamwise vortices tilted $\pm 4°$ in (x, z) plane (Fig. 12). These results agree well with those obtained from their two-point correlation $R_{\omega_x\omega_x}(\Delta x, \Delta z; y^+ = 20)$ where ω_x is the streamwise vorticity. They found that coherent structures tilting in (x, z)-planes due to mutual induction of overlapping vortices is responsible for kinked low-speed streaks and internal shear layers with negative $\partial u/\partial x$. The presence of that shear layer may be detected by using the VITA technique. In this detection scheme, the short-time variance of the velocity and the wall shear stress signals over an averaging time is calculated here, and an event is considered to occur when it exceeds a chosen threshold. The simultaneous conditional averages of the streamwise velocity at $y^+ = 5$ and the wall shear stress normalized by the local rms-values are shown in Fig. 13. It is clear from Fig. 13 that the LDV probe detects the events ahead of the shear probe. The fact that the shear-layer is seen earlier above the LDV measurement volume indicates a forward leaning structure in the (x, y)-plane. Fig. 13 gives an overall picture of the development of the shear-layer structure. The positive and negative $\partial\langle u\rangle/\partial t$ and $\partial\langle\tau\rangle/\partial t$ are interpreted by Jeong et al. [20] as being the result from the mutual induction by quasi-streamwise structures with positive ω_x and structures with negative ω_x because of their tilting in (x, z)-plane and overlap in the normal (x, y)-plane facilated by their inclination. Structure C in Fig. 12 induces motion toward the wall, leading to a positive $\langle u\rangle$ (sweep) in Fig. 13, while structure D induces velocity away from the wall, leading to a negative $\langle u\rangle$ (ejection) in Fig. 13.

This study shows that direct numerical simulations associated with the electrochemical method may open the opportunity of obtaining precious information about time dependent characteristics of the turbulence in the viscous wall region. In particular, this method should be a useful tool to test a given control of strategy.

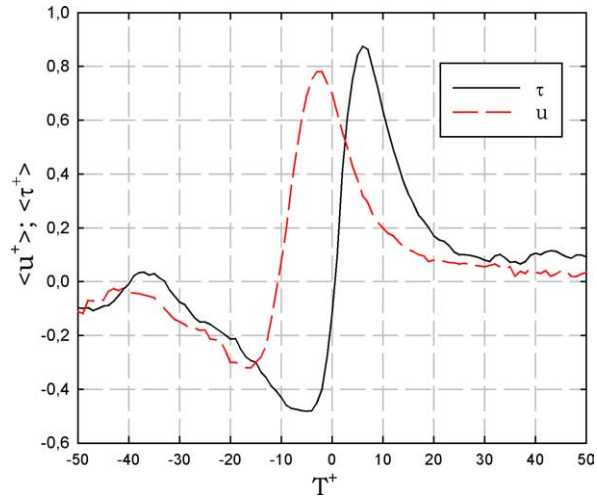

Fig. 13. Conditional averages of the positive VITA events of u and τ.

5. Conclusion

The transverse spacing between streaks (λ^+) was estimated by means of the space–time correlations using simultaneous measurements of velocity and wall shear stress on two points in the (y, z) plane. In the vicinity of the wall ($y^+ < 10$), $\lambda^+ = 110$ whereas for $y^+ > 10$, it increases with the wall distance, in accordance with the results found in the literature. An electrochemical probe array was designed and realized in order to study the spanwise cross-correlation between the wall shear stress provided by two probes of that the sensor array. The high spatial resolution of this device allows confirmation of the results found by the space–time correlations of the wall shear stress simultaneously measured at various points along the transverse axis (Z). Some curves of the space–time correlations reveal the existence of double peaks indicating that the quasi-streamwise structures were $\pm 6^\circ$ tilted in (x, z)-plane in accordance with the model suggested by Jeong et al. [20] who found that the quasi-steamwise structures are responsible for the streaks' formation, which in their turn cause the vortex regeneration, in accordance with the model of Hamilton and Weleffe [18]. It is confirmed that coherent structures tilting in (x, z)-plane is responsible for internal shear layers with positive $\partial u/\partial t$, commonly found by conditional averages. The present results could be used to improve some new strategies for the turbulent flow control in the near wall region by acting on the streak instability. This study indicates a potential usefulness of electrochemical sensors to analyse coherent structures of a turbulent boundary layer.

References

[1] F.R. Hama, Boundary layer characteristics for smooth and rough surfaces, in: Soci. Nava. Arch. Mar. Eng. Meeting Annual, New York, 1954, pp. 333–358.
[2] P.G. Runstadler, S.J. Kline, W.C. Reynolds, An experimental investigation of flow structure of the turbulent boundary layer, Rep. No. MD-8, Department Mech. Engrg., Stanfort University, Stanford, CA, 1963.
[3] H.P. Bakewell, J.L. Lumley, Viscous sublayer and adjacent wall region in turbulent pipe flow, Phys. Fluids 10 (1967).
[4] S.J. Kline, W.C. Reynold, F. Schraub, P.W. Rundstander, The structure of turbulent boundary layer, J. Fluid Mech. 30 (1967) 741–773.
[5] H.T. Kim, S.J. Kline, W.C. Reynolds, The production of turbulence near a smooth wall in turbulent boundary layer, J. Fluid Mech. 50 (1971) 133–160.
[6] A.K. Gupta, J. Laufer, R.E. Kaplan, Spatial structure in the viscous sublayer, J. Fluid Mech. 5 (1971) 493–512.
[7] J.M. Wallace, R.S. Brodkey, H. Eckelmann, Pattern-recognized structures in bounded turbulent shear flows, J. Fluid Mech. 83 (1977) 673–693.
[8] H.P. Kreplin, H. Eckelmann, Propagation of perturbations in the sublayer and adjacent wall region, J. Fluid Mech. 95 (1979) 305–322.
[9] C.R. Smith, S.P. Metzler, The characteristics of low-speed streaks in the near-wall region of a turbulent boundary layer, J. Fluid Mech. 129 (1983) 27–54.
[10] F.A. Schraub, S.J. Kline, A study of the structure of the turbulent boundary layer with and without long pressure gradients, Rep. MD-12, Deptartment Mech. Engrg., Standford University, CA, 1965.
[11] H. Nakagawa, I. Nezu, Structure of space–time correlations of bursting phenomena in an open-channel flow, J. Fluid Mech. 104 (1981) 1–43.

[12] R.F. Blackwelder, H. Eckelmann, Streamwise vortices associated with the burst phenomenon, J. Fluid Mech. 94 (1979) 577.
[13] D.D. Stretch, Automated pattern eduction from turbulent flow diagnostics, Annual Research Briefs, Center for Turbulence Research, Standford University, 1990, pp. 145–157.
[14] D.K. Oldaker, W.G. Tiederman, Spatial structure of the viscous sublayer in drag-reducing channel flows, Phys. Fluids Suppl. II 20 (10) (1977) 133–144.
[15] J. Kim, P. Moin, R.D. Moser, Turbulence statistics in fully developed channel flow at low Reynolds number, J. Fluid Mech. 177 (1987) 133–166.
[16] R.J. Adrian, C.D. Menhart, C.D. Tomkins, Vortex organization in the outer region of the boundary layer, J. Fluid Mech. 422 (2000) 1–54.
[17] J. Jiménez, P. Moin, The minimal flow unit in near-wall turbulence, J. Fluid Mech. 225 (1991) 213–240.
[18] J.M. Hamilton, J. Kim, F. Waleffe, Regeneration mechanisms of near-wall turbulence structures, J. Fluid Mech. 287 (1995) 317–348.
[19] F. Waleffe, Exact coherent structures in channel flow, J. Fluid Mech. 435 (2001) 93–102.
[20] J. Jeong, F. Hussain, W. Schoppa, J. Kim, Coherent structures near the wall in a turbulent channel flow, J. Fluid Mech. 332 (1997) 185–214.
[21] L. Labraga, B. Lagraa, A. Mazouz, L. Keirsbulck, Propagation of shear-layer structures in the near-wall region of a turbulent boundary layer, Exp. Fluids 33 (5) (2002) 670–676.
[22] A. Wietrzak, R.M. Lueptow, Wall shear stress and velocity in a turbulent axisymmetric boundary layer, J. Fluid Mech. 259 (1994) 191–218.
[23] J.E. Mitchell, T.J. Hanratty, A study of turbulence at wall using an electrochemical wall shear stress meter, J. Fluid Mech. 26 (1966) 199–221.
[24] C. Nikolaides, K.K. Lau, T.J. Hanratty, A study of the spanwise structure of coherent eddies in the viscous wall region, J. Fluid Mech. 130 (1983) 91–108.
[25] L.P. Reiss, T.J. Hanratty, Measurement of instantaneous rates of mass transfer to a small sink on a wall, AIChE J. 9 (1963) 154–160.
[26] T.J. Hanratty, J.A. Campbell, Measurement of wall shear stress, in: R.J. Goldstein (Ed.), Fluid Mechanics Measurements, Hemisphere, Washington, 1983, pp. 559–615.
[27] M. Lebouché, Contribution à l'étude des mouvements turbulents par la méthode polarographique, Thèse de Docteur des Sciences, Université de Nancy, 1968.
[28] G. Fortuna, T.J. Hanratty, Frequency response of the boundary layer on the wall transfer probes, Int. J. Heat Mass Transfer. 14 (1971) 1499–1507.
[29] C. Deslouis, O. Gil, B. Tribollet, Frequency response of electrochemical sensors to hydrodynamic fluctuations, J. Fluid Mech. 215 (1990) 85–100.
[30] T. Maquinghen, Métrologie tridimensionnelle instationnaire à l'aide de la méthode polarographique, Thèse de Doctorat, Université de Valenciennes, 1999.
[31] V. Sobolik, O. Wein, J. Cermak, Simultaneous measurement of film thickness and wall shear stress in way flow on non-Newtonian liquids, Collect. Czech Chem. Commun. 52 (1987) 913–928.
[32] O. Wein, On the transient Leveque's problem with application in electrochemistry, Collect. Czech Chem. Commun. 46 (1981) 3209–3220.
[33] B. Lagraa, Interaction entre les mouvements à grandes échelles et les structures pariétales dans une couche limite turbulente, Thèse de doctorat à l'Université de Valenciennes, 2002.
[34] C.R. Smith, A synthesized model of the near-wall behavior in turbulent boundary layer, in: Proc. Symp. Turbul., 8th, Rolla, MO, 1984.
[35] S.K. Robinson, Coherent motions in the turbulent boundary layer, Annu. Rev. Fluid Mech. 23 (1991) 601–639.
[36] M.K. Lee, L.D. Eckelman, T. Hanratty, Identification of turbulent wall eddies through the phase relation of the components of the fluctuating velocity gradient, J. Fluid Mech. 66 (1974) 17–33.